Developmental Cell
Article

Synaptojanin 1-Mediated PI(4,5)P_2 Hydrolysis Is Modulated by Membrane Curvature and Facilitates Membrane Fission

Belle Chang-Ileto,[1] Samuel G. Frere,[1] Robin B. Chan,[1] Sergey V. Voronov,[1] Aurélien Roux,[2] and Gilbert Di Paolo[1,*]
[1]Department of Pathology and Cell Biology, Taub Institute for Research on Alzheimer's Disease and the Aging Brain, Columbia University Medical Center, New York, NY 10032, USA
[2]Biochemistry Department, University of Geneva, Science II, CH-1211 Geneva 4, Switzerland
*Correspondence: gil.dipaolo@columbia.edu
DOI 10.1016/j.devcel.2010.12.008

SUMMARY

Phosphatidylinositol-4,5-bisphosphate [PI(4,5)P_2] plays a fundamental role in clathrin-mediated endocytosis. However, precisely how PI(4,5)P_2 metabolism is spatially and temporally regulated during membrane internalization and the functional consequences of endocytosis-coupled PI(4,5)P_2 dephosphorylation remain to be explored. Using cell-free assays with liposomes of varying diameters, we show that the major synaptic phosphoinositide phosphatase, synaptojanin 1 (Synj1), acts with membrane curvature generators/sensors, such as the BAR protein endophilin, to preferentially remove PI(4,5)P_2 from curved membranes as opposed to relatively flat ones. Moreover, in vivo recruitment of Synj1's inositol 5-phosphatase domain to endophilin-induced membrane tubules results in fragmentation and condensation of these structures largely in a dynamin-dependent fashion. Our study raises the possibility that geometry-based mechanisms may contribute to spatially restricting PI(4,5)P_2 elimination during membrane internalization and suggests that the PI(4,5)P_2-to-PI4P conversion achieved by Synj1 at sites of high curvature may cooperate with dynamin to achieve membrane fission.

INTRODUCTION

Phosphatidylinositol-4,5-bisphosphate [PI(4,5)P_2] is a phosphoinositide that is concentrated in the cytosolic leaflet of the plasma membrane, where it plays a primary role in the regulation of a large number of biological functions, including signal transduction, cytoskeletal dynamics, ion permeability and traffic to and from the cell surface (Di Paolo and De Camilli, 2006). Consistent with its multiple roles in cell physiology, PI(4,5)P_2 is subject to tight regulation through a variety of lipid enzymes, such as phospholipases, phosphatidylinositol phosphate kinases and inositol 4- and 5-phosphatases. Thus, a fundamental question is how the metabolism of PI(4,5)P_2 is coordinated and spatially restricted to ensure the appropriate distribution of PI(4,5)P_2 levels at the membrane, in order to simultaneously mediate these complex processes within the same cell (Di Paolo and De Camilli, 2006; McLaughlin and Murray, 2005). A partial answer may be provided by reports that PI(4,5)P_2 appears to be nonuniformly distributed at the plasma membrane in the form of microdomains (Chichili and Rodgers, 2009; Milosevic et al., 2005; Pike, 2009), though reports to the contrary also exist (van Rheenen et al., 2005). These putative microdomains may restrict access by PI(4,5)P_2 metabolizing enzymes that are themselves regulated by a variety of mechanisms, including phosphorylation, dephosphorylation, and interactions with binding partners mediating their subcellular targeting (Di Paolo and De Camilli, 2006).

The essential nature of PI(4,5)P_2 homeostasis has been demonstrated by studies on clathrin-mediated endocytosis. Indeed, PI(4,5)P_2 functions in endocytosis, at least in part, to recruit and concentrate at the plasma membrane core components of the endocytic machinery, such as the clathrin adaptors AP-2, AP-180, and epsin (Di Paolo and De Camilli, 2006; Traub, 2005). Additional factors that regulate fundamental aspects of the endocytic process, including the fission factor dynamin, bind to PI(4,5)P_2 and this interaction appears to be critical for their function (Jost et al., 1998; Ramachandran and Schmid, 2008). Importantly, characterization of the main PI(4,5)P_2 5-phosphatase in the brain, synaptojanin 1 (Synj1), has indicated that PI(4,5)P_2 dephosphorylation is essential for the proper recycling of synaptic vesicles at neuronal synapses in mice. For instance, a decreased ability to hydrolyze PI(4,5)P_2 was shown to cause pleiotropic phenotypes, such as the accumulation of clathrin-coated vesicles and other aberrant endocytic intermediates as well as slower rates of synaptic vesicle endocytosis and recycling in *Synj1*$^{-/-}$ neuronal synapses (Cremona et al., 1999; Hayashi et al., 2008; Kim et al., 2002; Mani et al., 2007). Similar observations were made in synapses from the worm (Harris et al., 2000) and the fly (Verstreken et al., 2003). In budding yeast, lack of synaptojanin-like proteins results in alterations of the actin cytoskeleton and of the endocytic process (Singer-Kruger et al., 1998; Srinivasan et al., 1997; Stefan et al., 2002, 2005; Sun et al., 2007). Together, these studies on synaptojanin family members in various model organisms have established a primary and evolutionarily conserved role for these phosphoinositide phosphatases in endocytosis.

Synj1 occurs as two main isoforms, a brain-enriched 145 kDa protein (Synj1-145) and a ubiquitously expressed 170 kDa

protein (Synj1-170), which both share an NH_2-terminal Sac1 region, a central inositol 5-phosphatase domain and a COOH-terminal proline-rich domain (PRD) (McPherson et al., 1996). Although the Sac1 domain can dephosphorylate a variety of phosphoinositides in vitro (Guo et al., 1999), its physiological substrate(s) remain(s) unknown. Conversely, the 5-phosphatase domain has been extensively characterized and shown to use PI(4,5)P_2 as its primary substrate to mediate PI(4,5)P_2-to-PI4P conversion (Cremona et al., 1999; McPherson et al., 1996). This latter property is believed to be central to the physiological actions of Synj1 (Cremona et al., 1999; Mani et al., 2007). While a role of Synj1-170 in endocytosis has not been clearly demonstrated, overwhelming evidence has been reported indicating a primary role of Synj1-145 (hereafter referred to as Synj1) in clathrin-mediated endocytosis in the adult brain.

At synapses, Synj1 is predominantly recruited to sites of endocytosis by the Src homology 3 (SH3) domain-containing protein, endophilin (Gad et al., 2000; Ringstad et al., 1997), although various other endocytic SH3 proteins have been reported to interact with Synj1, such as amphiphysin and intersectin (Dittman and Ryan, 2009). The physiological relevance of this partnership is supported by results from proline-rich synaptojanin peptide injections in the giant synapse of the lamprey (Gad et al., 2000), genetic studies in the fly and the worm (Schuske et al., 2003; Verstreken et al., 2003), and the fact that an endophilin-binding deficient mutant of Synj1 largely fails to rescue synaptic trafficking defects in cultured *Synj1*$^{-/-}$ neurons (Mani et al., 2007). An important feature of endophilin family members is that they contain a Bin1/ Amphiphysin/ Rvs (BAR) domain, which exhibits at least four key properties (Frost et al., 2009; Peter et al., 2004): (1) binding to acidic phospholipids; (2) domain homo/heterodimerization; (3) evagination of liposomes into narrow tubules in a process that is potentiated by its NH_2-terminal amphipathic helix; and (4) sensing of membrane curvature via its crescent-shaped structure, with a preference for highly curved, synaptic- (or endocytic-)like vesicles. While endophilin's relatively late recruitment to clathrin-coated pits (i.e., at a time immediately preceding the fission process) argues against a primary role of the tubulating activity of its BAR domain in the budding process, it may be involved in stabilizing membrane curvature at sites of endocytosis, potentially in concert with other BAR proteins and/or the fission factor, dynamin (Perera et al., 2006).

In this study, we investigate the potential membrane curvature-based mechanism by which PI(4,5)P_2 metabolism may be regulated during the endocytic process as well as the significance of this PI(4,5)P_2 hydrolysis on areas of high curvature, such as endocytic bud necks. Our results from cell-free experiments indicate that the balance between PI(4,5)P_2 synthesis and elimination is regulated by membrane curvature, with more efficient hydrolysis achieved by the Synj1-endophilin partnership on highly curved liposomes compared with relatively flat liposomes. Furthermore, we show that acute induction of PI(4,5)P_2-to-PI4P conversion on highly curved, endophilin-coated membrane tubules promotes membrane fragmentation largely in a dynamin-dependent fashion, suggesting that this lipid change may cooperate with dynamin to facilitate the membrane fission process.

RESULTS

PI(4,5)P_2 Metabolism Is Affected by the Size of Substrate Liposomes

Since the main PI(4,5)P_2 phosphatase in the brain is Synj1 (Cremona et al., 1999; Voronov et al., 2008) and its main physiological partner is the BAR-domain protein endophilin (Gad et al., 2000; Ringstad et al., 1997; Schuske et al., 2003; Verstreken et al., 2003), we hypothesized that this partnership may function to facilitate PI(4,5)P_2 hydrolysis on highly curved membranes, thereby resulting in the robust elimination of PI(4,5)P_2 from invaginating membranes during the endocytic process. Indeed, the BAR domain of endophilin, similar to that of amphiphysin, has been shown to preferentially bind to highly curved membranes (i.e., 50 nm liposomes) over flatter membranes (i.e., 800 nm liposomes) (Gallop et al., 2006; Peter et al., 2004).

We tested the effect of membrane curvature on PI(4,5)P_2 metabolism using rat brain cytosol incubated with liposomes (derived from brain lipids) of varying sizes (i.e., 800, 400, 100, and 50 nm) (Figure 1A) and in the case of 800 and 50 nm liposomes, of similar lipid composition (see Figures S1A–S1C available online). The liposome panel, identified by the membrane pore size used for extrusion, was subjected to a modified phospholipid radiolabeling assay that measures activity levels of PIP2, PIP, and PA metabolizing enzymes (Figure 1B) (Cremona et al., 1999; Di Paolo et al., 2004). Phospholipids from the liposomes were separated by thin layer chromatography (TLC) and levels of incorporated radiolabel were quantified by phosphorimaging (Figures 1B and 1C). In previous studies using this method, it was shown that the predominant radiolabeled PIP_2 species generated was PI(4,5)P_2 while the PIP fraction consisted of both PI3P and PI4P (Cremona et al., 1999). Results show that 50 nm liposomes had 68.2% ± 1.0% of PIP_2 radiolabeling and 66.1% ± 1.5% of PIP2/PIP ratio compared with 800 nm liposomes ($n = 34$, $p < 0.001$). Furthermore, the levels of radiolabeled PIP_2 decreased with decreasing liposome diameter while PIP levels remained the same and PA levels showed a modest increase (Figures 1C and 1D; Figure S2A). Further decreasing the liposome diameter to ~30 nm did not give PIP_2 values significantly different than those from 50 nm membranes (data not shown). The level of radiolabeling of PIP_2 in this assay suggests that there are PIP_2 metabolizing enzymes present in the brain that are sensitive to the level of curvature and/or lipid packing, resulting in the differential labeling of PIP_2 on the different size liposomes.

The Effect of Liposome Size on PI(4,5)P_2 Metabolism Is Mediated by Synj1 and Endophilin

To determine whether Synj1 mediates the decrease in PI(4,5)P_2 radiolabeling observed with small liposomes (Figure 1), we utilized brain cytosol from *Synj1*$^{-/-}$ mice (Figure 2A) in the phospholipid radiolabeling assay. Consistent with previous work (Cremona et al., 1999; Di Paolo et al., 2004; Voronov et al., 2008), *Synj1*$^{-/-}$ cytosol had a dramatically decreased ability to hydrolyze water-soluble fluorescently labeled PI(4,5)P_2 relative to control cytosol (Figure 2B). While the wild-type cytosol shows liposome size-dependent labeling of PIP_2 as described above, *Synj1*$^{-/-}$ cytosol did not, suggesting that Synj1 mediates increased PI(4,5)P_2 catabolism on small, highly curved

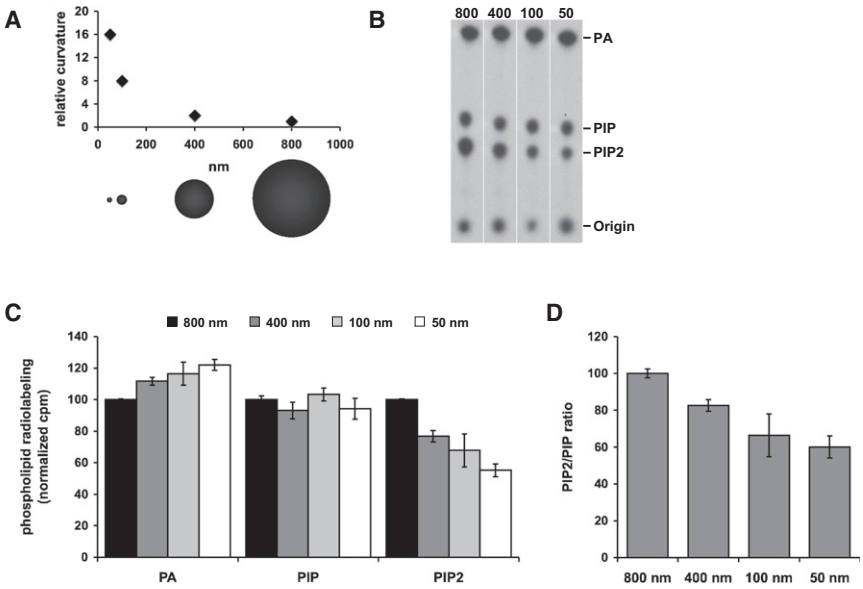

Figure 1. PIP_2 Metabolism Is Affected by the Size of Substrate Liposomes

(A) Relationship between the liposome diameter and relative curvature. The diameters illustrated are those of the membrane pores through which extrusion of liposomes were performed and thus reflect the theoretical diameters of liposomes used. For actual measured diameters, see Supplemental Experimental Procedures.

(B) Autoradiography of a TLC showing levels of incorporated radiolabeling on phospholipids when liposomes were incubated with brain cytosol in the presence of [γ-^{32}P]-ATP.

(C) Quantification of phospholipid radiolabeling by phosphorimaging. The counts of PIP2, PIP, and PA were normalized to that of 800 nm.

(D) The ratio of PIP_2/PIP for the different sized liposomes. n = 6 for 800 and 50 nm, n = 4 for 400 and 100 nm. Data are represented as mean ± SEM. See also Figure S1.

liposomes (Figure 2C). Next, we performed biochemical depletion of Synj1 and endophilin from wild-type cytosol to study the effects of removing these proteins on the membrane curvature-dependent labeling of PIP_2. The SH3 domain of endophilin expressed as a GST-fusion protein was used to biochemically deplete Synj1 and dynamin, another major interacting protein of endophilin, from normal cytosol (Figure 2D). This Synj1- and dynamin-depleted cytosol, like the *Synj1*$^{-/-}$ cytosol, lost its ability to preferentially hydrolyze PIP_2 from small liposomes (Figure 2E). Since endophilin is the major physiological protein interactor of Synj1 and is responsible for recruiting Synj1 to membranes (Gad et al., 2000; Ringstad et al., 1997; Schuske et al., 2003; Verstreken et al., 2003), endophilins were biochemically depleted from normal cytosol using the proline-rich domain (PRD) of Synj1 and dynamin fused to GST. Western blots of the depleted cytosol showed that while endophilin was quantitatively depleted from the cytosol (Figure 2D), other BAR proteins, such as amphiphysin 1 (data not shown) were not. Use of the PRD-depleted cytosol also showed the disappearance of the membrane curvature effect (Figure 2E). While the membrane curvature sensitivity of the PIP2/PIP ratio disappeared in the absence of Synj1 and endophilin, the higher PA/PIP ratio on the small diameter liposomes was unaffected despite the absence of these proteins (Figures S1D–S1F). Taken together, these data suggest that the increased catabolism of $PI(4,5)P_2$ observed on small, highly curved liposomes is primarily mediated by the proteins Synj1 and endophilins.

Synj1 Preferentially Hydrolyzes $PI(4,5)P_2$ on Small Liposomes

Next, investigation of the recruitment of Synj1 protein from brain cytosol to 800 and 50 nm liposomes in sedimentation assays revealed that the binding of this inositol phosphatase increased 52% ± 10% on 50 nm liposomes over 800 nm liposomes after incubation at 4°C (Figures 3A and 3B) and a similar increase was observed at 37°C (data not shown). In the same reactions, dynamin and endophilin showed no binding preference for different sized liposomes. One effect of this differential recruitment of Synj1 is that the Synj1/endophilin protein ratio was 44% ± 8% higher on 50 nm liposomes when compared with 800 nm liposomes while the dynamin/ endophilin ratio remained the same (Figure 3C). In similar experiments using endophilin-depleted cytosols, the recruitment of Synj1 to liposomes was dramatically decreased (data not shown).

To determine whether the ability of Synj1 to hydrolyze $PI(4,5)P_2$ was also affected by liposome size, a time course measuring free phosphate was used to track the levels of released phosphate upon liposome incubation with Synj1 in the presence or absence of endophilin (Figure 3D). Results show that the amount of phosphate released by Synj1 was increased by ~30% on the 50 nm liposomes relative to 800 nm liposomes after 60 min incubation (Figure 3D; Table S1). However, the estimated initial rate of phosphate release by Synj1 alone was not influenced by liposome size. Importantly, while the activity of Synj1 was unaffected by endophilin on the 800 nm liposomes, there was a significant increase on the 50 nm liposomes in the presence of endophilin with the estimated initial rate increasing ~90% over that of Synj1 alone on 800 nm liposomes or 50% over that of Synj1 alone on 50 nm liposomes (Figures 3D; Figure S2A and Table S1). In addition, there was a ~65% increase in phosphate release from 50 nm liposomes by Synj1 in the presence of endophilin relative to Synj1 alone from 800 nm liposomes or ~25% increase relative to Synj1 alone from 50 nm (Figure 3D; Table S1). In order to resolve whether the increase in Synj1 activity in the presence of endophilin was caused by the direct interaction of these two endocytic proteins, the same time-course analyses were performed with a Synj1 defective in its binding to endophilin through point mutations in its PRD domain (endophilin-binding deficient mutant of Synj1, or Synj1-EBD) (Gad et al., 2000; Mani et al., 2007; Ringstad et al., 2001). Endophilin failed to increase the rate of $PI(4,5)P_2$ hydrolysis by the Synj1-EBD mutant (Figure S2B). Results from time-course studies using 30 nm liposomes yielded similar results as those using 50 nm liposomes (data not shown).

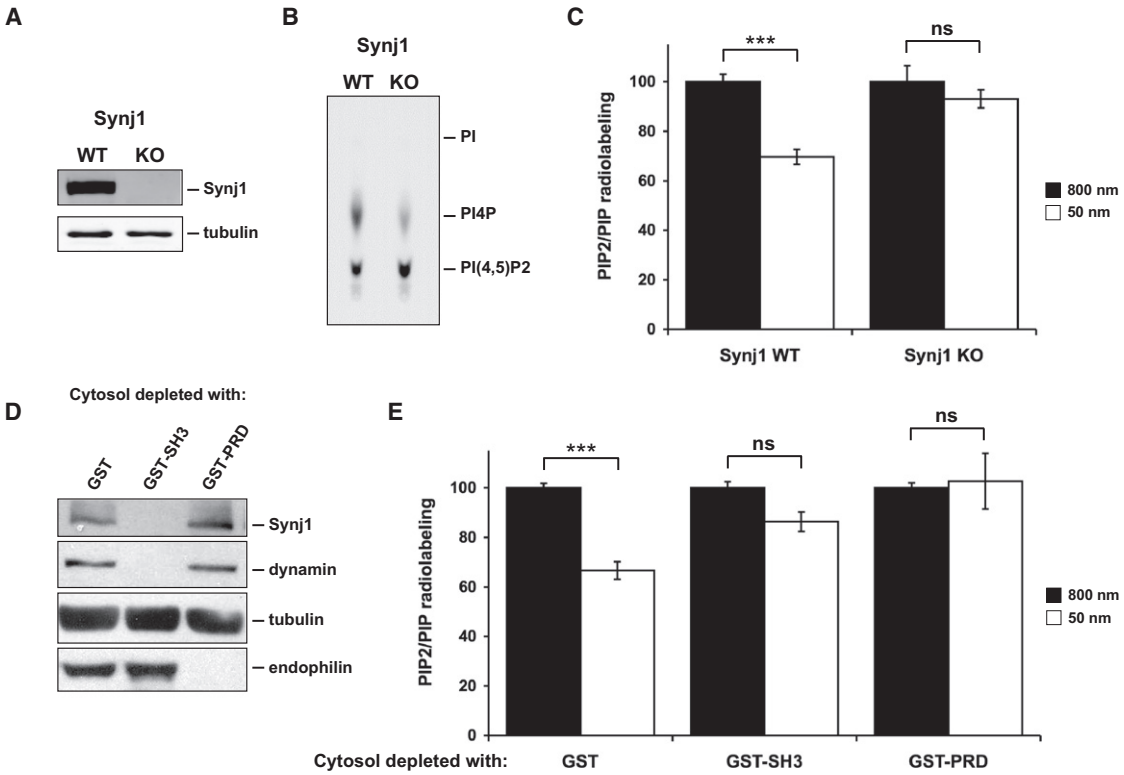

Figure 2. The Curvature Effect in PIP_2 Metabolism Is Mediated by the Proteins Synj1 and Endophilin

(A) Western blot of brain cytosol from *Synj1*$^{+/+}$ (WT) and *Synj1*$^{-/-}$ (KO) newborn mice.

(B) Analysis of the hydrolysis of soluble $PI(4,5)P_2$ when incubated with brain cytosol from Synj1$^{+/+}$ and *Synj1*$^{-/-}$ newborn mice.

(C) The ratio of PIP_2/PIP when 800 and 50 nm liposomes are incubated with brain cytosol from *Synj1*$^{+/+}$ (WT) and *Synj1*$^{-/-}$ (KO) newborn mice in the phospholipid radiolabeling assay.

(D) Western blot on the rat brain cytosols depleted of either Synj1 (using recombinant SH3 domain of endophilin fused to GST, which also results in the removal of dynamin) or endophilin (using recombinant PRD domains of both Synj1 and dynamin 1 fused to GST).

(E) The ratio of PIP_2/PIP when 800 and 50 nm liposomes are incubated with the biochemically depleted cytosols. Data are represented as mean ± SEM. ***$p < 0.001$; n = 6 in C) and n = 6–10 in E). See also Figure S1.

These data with purified components show that Synj1 hydrolyzes $PI(4,5)P_2$ more efficiently on small substrate liposomes and that Synj1's activity is potentiated by direct interaction with endophilin specifically on small liposomes. These results also expand on previous studies showing that the SH3 domain of endophilin enhances the activity of Synj1 on water soluble $PI(4,5)P_2$ (Lee et al., 2004).

To test if the intrinsic ability of Synj1 to hydrolyze $PI(4,5)P_2$ from small liposomes simply stems from its higher levels of recruitment to these membranes or whether this enzyme can actually distinguish membrane curvature and/or lipid packing defects, the levels of Synj1 recruitment to liposomes of different sizes were artificially equalized. This was achieved through the incorporation of a synthetic lipid dioleoyl-glycero-succinate (DGS) containing a nitroloactic acid-nickel salt (NiNTA) label into the different sized liposomes that allowed the controlled recruitment of histidine-tagged (His-tagged) proteins, in this case, His-tagged Synj1 (His-Synj1) to these liposomes. In order to measure activity of the His-Synj1, fluorescently labeled $PI(4,5)P_2$ (BODIPY-$PI(4,5)P_2$) was also included on these liposomes. With the NiNTA label, His-Synj1 was recruited equally to 800 and 50 nm liposomes and this recruitment could be significantly blocked with the divalent cation chelating agent EDTA (Figures S2C and S2D). Assessment of $PI(4,5)P_2$ hydrolysis activity (Figure 3E; Figure S2E) showed that despite the equal recruitment of Synj1 to both 800 and 50 nm liposomes, $PI(4,5)P_2$ hydrolysis was greater on the smaller liposomes. When the recruitment of His-Synj1 was blocked by EDTA, the differences seen in $PI(4,5)P_2$ hydrolysis disappeared. Thus, higher levels of $PI(4,5)P_2$ hydrolysis from small liposomes may result not only from the higher levels of Synj1 recruitment to these membranes but also from Synj1's intrinsic preference for highly curved membranes or the lipid packing defects that arise from the membrane deformation at these high curvatures.

Characterization of Endophilin Lipid and Membrane Binding Properties

While a curvature-based mechanism may account for robust hydrolysis of $PI(4,5)P_2$ during membrane internalization and a corresponding efficient elimination of this lipid from intracellular organelles along the endocytic pathway, it may also have an impact on membrane dynamics during endocytosis (Liu et al., 2009). Indeed, the spatially restricted and rapid change in $PI(4,5)P_2$/PI4P composition may affect the biophysical and/or

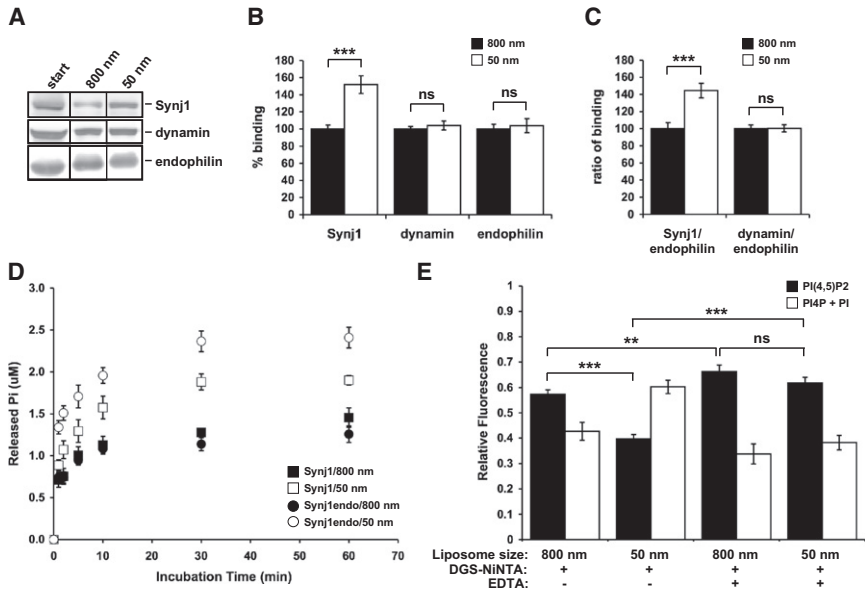

Figure 3. Synj1 Preferentially Hydrolyzes PI(4,5)P_2 on High Curvature Membranes

(A) Western blot analysis and (B) quantification by infrared detection of Synj1, endophilin and dynamin recruitment to membranes when brain cytosol is incubated with 800 and 50 nm liposomes.

(C) Normalization of Synj1 and dynamin to endophilin levels.

(D) Time course of PI(4,5)P_2 hydrolysis by Synj1 using measurements of free phosphate when 800 or 50 nm liposomes are incubated with recombinant Synj1 (12 nM) in the presence or absence of recombinant endophilin (120 nM).

(E) Measurement of BODIPY- PI(4,5)P_2 hydrolysis in conditions where His-Synj1 recruitment is equalized using NiNTA liposomes. Data are represented as mean ± SEM. ***$p < 0.001$; **$p < 0.01$; n = 12 in (B) and (C), n = 4 in (D), and n = 15 in (E). See also Figure S2 and Table S1.

signaling properties of invaginating membranes. Based on recent evidence indicating that Synj1 is recruited to endocytic pits concomitantly with endophilin and dynamin immediately prior to the fission process (Perera et al., 2006), that a PI(4,5)P_2 probe is shed from endocytic membranes before they undergo scission (Sun et al., 2007), and that the rate of endocytosis is decreased in *Synj1*$^{-/-}$ synapses (Mani et al., 2007), a role for PI(4,5)P_2 hydrolysis in facilitating the fission process is plausible. We reasoned that the most direct way to test this idea is to assess the consequences of rapid PI(4,5)P_2 changes on endophilin-induced tubules and as a precursor to these experiments, to characterize the lipid-binding and membrane-tubulating properties of endophilin, in vitro and in intact cells, respectively.

The interaction of endophilin 1 with membrane bilayers containing anionic phospholipids is driven by electrostatic interactions such that high salt concentrations can decrease the binding to membranes (Gallop et al., 2006). Recruitment of the various domains of endophilin 1 to a panel of phospholipids was tested (Figure 4A; Figure S3). While the BAR domain alone showed no distinct preference for the various phospholipids, full-length endophilin 1 was preferentially recruited to the more highly phosphorylated lipids, a property that was recapitulated by the N-BAR domain (i.e., the BAR domain preceded by the NH_2-terminal amphipathic helix) (Masuda et al., 2006; Peter et al., 2004; Weissenhorn, 2005). Grouping the phosphoinositides according to the level of phosphorylation [i.e., PI3P, PI4P, and PI5P are classified as monophosphorylated PIs (monoPi)] shows that endophilin binding to the lipids increased as the number of phosphates on the inositol ring increases (Figure 4A; Figure S3). While F-BAR proteins have been reported to depend on the presence of PS, a phospholipid abundant at the plasma membrane, for binding to bilayer membranes (Itoh et al., 2005), experiments with endophilin showed significant binding to PI(4,5)P_2 liposomes that was enhanced by but did not require the presence of PS (Figure 4B). Thus, the binding of endophilin to liposomes increases as the anionic charge of the phosphoinositide increases and is modulated by PS.

Overexpression of endophilin in COS-7 cells induces considerable tubulation of cellular membranes (Figure S3C). Since we found that endophilin binds more strongly to highly phosphorylated PIs and since PI(4,5)P_2 is the predominant phosphoinositide found at the plasma membrane, we examined the distribution of this lipid in cells overexpressing endophilin. Coexpression of endophilin with the PI(4,5)P_2 probe PLCδ1-PH (Hurley and Meyer, 2001) showed that the tubules induced by endophilin overexpression are enriched in PI(4,5)P_2, similar to the plasma membrane (Figure 4C). Consistent with a primary role of PI(4,5)P_2 in the recruitment of endophilin, overexpression of PLCδ1-PH at higher levels and the resulting sequestration of this lipid blocks the tubulating activity of endophilin (data not shown). Since endophilin binds to membranes via electrostatic interaction between the basic residues lining its concave face and the anionic lipids in membranes, we investigated whether the membranes of the endophilin-induced tubules would be areas of high surface potential (i.e., areas containing a concentration of negative charge). Coexpression of the high surface potential probe, R-pre probe (McLaughlin and Murray, 2005; Yeung et al., 2006), with endophilin resulted in localization of the probe with the endophilin-induced tubules (Figure 4D). Finally, extracellular application of membrane impermeable fluorescent dye, FM4-64, shows that the vast majority of membrane tubules are accessible by the dye (Figure 4E). Together, these data suggest that endophilin-induced tubules are largely derived from the plasma membrane, have a high surface potential and are enriched in PI(4,5)P_2.

Induced PI(4,5)P_2 Dephosphorylation on Endophilin Tubules Results in Membrane Fission

Having determined that endophilin-coated tubules are enriched in PI(4,5)P_2, the impact of PI(4,5)P_2-to-PI4P conversion on membrane dynamics and specifically, membrane fission, can be assessed in intact cells. While endophilin mediates the recruitment of Synj1 via its SH3 domain and the PRD of the enzyme (Figures S3C and S3D) (see also Gad et al., 2000;

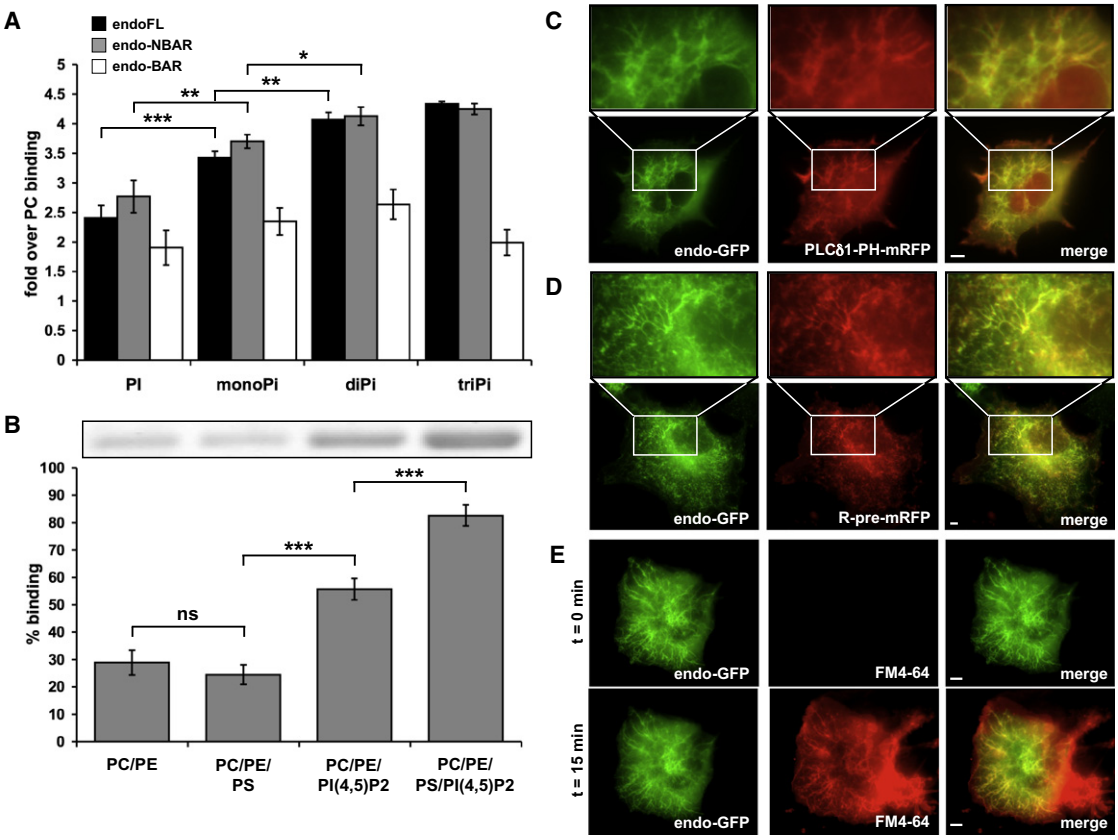

Figure 4. Endophilin Binds to Highly Phosphorylated Phosphoinositides and, upon Overexpression, Induces Tubules Originating from the Plasma Membrane that Are Enriched in PI(4,5)P_2

(A) Binding of endophilin domains (full-length, N-BAR and BAR) to phosphoinositides were evaluated using liposome sedimentation with a panel of liposomes composed of different phospholipids.

(B) Binding of full-length endophilin to PI(4,5)P_2 liposomes with or without PS.

(C) Coexpression of endophilin-GFP and the PLCδ1-PH-mRFP in COS-7 cells.

(D) Coexpression of endophilin-GFP with the surface potential marker R-pre-mRFP in COS-7 cells.

(E) Treatment of endophilin-GFP transfected cells with the lipophilic probe FM4-64 at t = 0 and 15 min. Data are represented as mean ± SEM. *$p < 0.05$, **$p < 0.01$, ***$p < 0.001$; n = 3 in (A) and n = 6 in (B). Scale bar = 5 μm. See also Figure S3.

Ringstad et al., 1997), consistent with the colocalization of these two proteins in neurons (Figure S3E), a method to temporally and spatially control the recruitment of Synj1 to endophilin-induced tubules was required. A general drug-inducible protein heterodimerization strategy takes advantage of the ability of various small molecules to bring together two different protein domains. In this paradigm, proteins and/or discrete domains of interest are fused to either the FK506-binding protein (FKBP) or a rapamycin-binding domain of mTOR (FRB) allowing heterodimerization upon addition of rapamycin or a chemical analog (rapalog). This approach has been used to target phosphoinositide phosphatases or kinases to the plasma membrane or endosomes (Haucke and Di Paolo, 2007; Nakatsu et al., 2010).

To utilize the rapamycin- or rapalog-induced heterodimerization approach, the 5-phosphatase domain of Synj1, either wild-type or the catalytically inactive version (Synj1-Ptase, Synj1-PtaseD730A, respectively) (Mani et al., 2007), was fused to the FKBP domain and the fluorescent tag mRFP while endophilin without the SH3 domain (endoΔSH3) was fused to the mutant FRB domain and the fluorescent tag EGFP (Figure 5A). The SH3 and PRD domains were not included in these fusions in order that interaction of these two heterologous proteins be spatially and temporally regulated exclusively by the heterodimerization paradigm. Coexpression of these two chimeric proteins in COS-7 cells resulted in endophilin-marked tubules that showed no recruitment of the Synj1 chimera, which was instead diffuse in the cytoplasm (Figures 5B–5D, pre-rapa and t = 0). Addition of the AP21967 rapalog to the media of these cotransfected COS-7 cells caused the recruitment of the Synj1-Ptase chimera to the endophilin-induced tubules (Figure 5B-C, post-rapa and t = 5 min) and was followed by at least two types of behavior: fragmentation and condensation of the tubules (Figures 5B and 5C; Movies S1–S3). These phenomena resulted in a ~60% reduction in tubule length (Figure 5E) and resemble the breakage and movement of tubules after latrunculin washout seen in a study of F-BAR proteins (Itoh et al., 2005). Addition of the AP21967 rapalog to cells coexpressing the catalytically inactive mutant Synj1-PtaseD730A chimera and endophilin chimera resulted in relocalization of the cytosolic Synj1-PtaseD730A to the endophilin-induced tubules but did

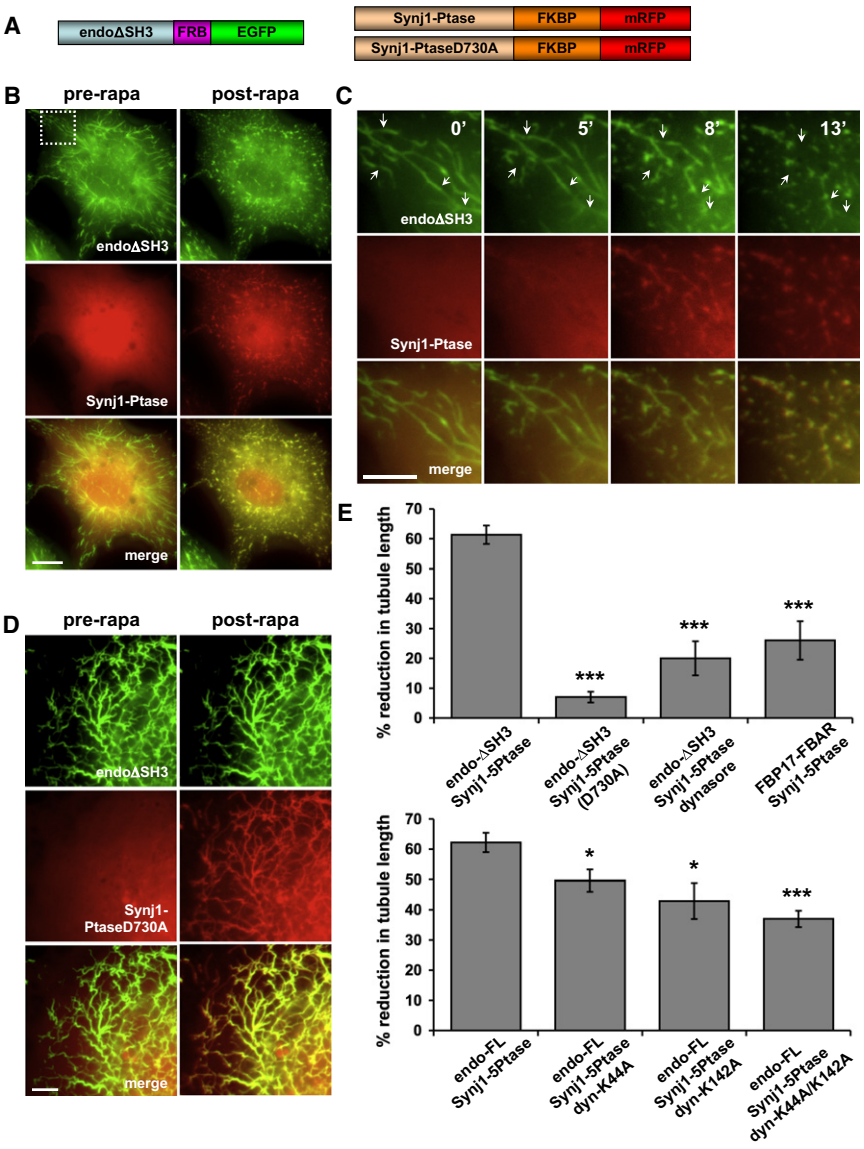

Figure 5. Acute Recruitment of the Inositol 5-Phosphatase Domain of Synj1 to Endophilin-Induced Tubules Results in Membrane Fragmentation and Condensation

(A) Diagram of the heterodimerization constructs: rat endophilin1 without the SH3 domain (endoΔSH3) is fused to the NH_2-terminal side of the FRB domain followed by EGFP; the inositol 5-phosphatase domain of Synj1, either wild-type or catalytically dead mutant D730A (Synj1-Ptase, Synj1-PtaseD730 respectively), is fused to the NH_2-terminal side of two FKBP domains followed by mRFP.

(B) In transfected COS-7 cells, Synj1-Ptase shows a diffuse signal before rapalog treatment (pre-rapa). Rapalog treatment results in Synj1-Ptase recruitment to endophilin-induced membrane tubules and fragmentation and condensation of the membrane tubules take place (post-rapa).

(C) A time-lapse view of the fragmentation and condensation events upon rapalog treatment from a magnified field of the cell seen in B) as indicated by the dotted square. Examples of fragmentation sites are indicated by the arrows.

(D) In transfected COS-7 cells, Synj1-PtaseD730A shows a diffuse signal before rapalog treatment (pre-rapa). Rapalog addition results in Synj1-PtaseD730A recruitment to endophilin-induced membrane tubules but no fragmentation/condensation events are observed (post-rapa).

(E) Reduction of tubule size as a measure of membrane fragmentation and condensation efficiency. To quantify the extent of membrane fission, tubule length before and after rapamycin/rapalog-treatment were measured. Data are represented as mean ± SEM. ***$p < 0.001$; *$p < 0.05$; from left to right, n = 24,9,5,6 (top graph); n = 7,8,9,22 (bottom graph). Scale bars represent (B) 10 μm, (C) 5 μm, and (D) 5 μm. See also Figure S3 and Movies S1–S4.

not result in fragmentation or condensation of the tubules (Figures 5D and 5E; Movie S4). Use of rapamycin in place of the AP21967 rapalog resulted in the same effects: recruitment of the Synj1 chimera to endophilin-induced tubules, albeit with faster kinetics, and, in the case of active Synj1, fragmentation and condensation of these tubules (data not shown).

To monitor the hydrolysis of $PI(4,5)P_2$ on endophilin-coated tubules, the heterodimerization experiment was performed using a mRFP-tagged PLCδ1-PH, in order to follow the presence of $PI(4,5)P_2$, and a nonfluorescently tagged Synj1-Ptase (Figure 6A). Before rapamycin addition, PLCδ1-PH localized to the endophilin-induced tubules, as expected (Figure 4C). After rapamycin treatment, the PLCδ1-PH translocated from the tubules to the cytosol, thus denoting $PI(4,5)P_2$ hydrolysis (Figure 6A; Movies S5 and S6). In addition, a membrane-impermeable amphipathic fluorescent probe, FM4-64, was used to follow the membrane remodeling dynamics during the observed fission phenomenon to rule out that the disappearance of tubules is merely a result of endophilin falling off the tubules (Figure 6B). Again, a nonfluorescently tagged Synj1-Ptase was used and cells were exogenously treated with FM4-64 to label the tubules as in Figure 4E. Upon rapamycin treatment, fragmentation/ condensation of the tubules were observed with the FM4-64 labeling indicating that the membrane tubules were undergoing reorganization. However, in cases where fat tubular structures (likely corresponding to large bundles of tubules) were present, FM fluorescence resisted the phosphatase treatment (unlike the endophilin fluorescence; data not shown). Last, whether tubules induced by other membrane-deforming proteins can produce the same fragmentation/condensation phenomenon was examined. Overexpression of the F-BAR domain of FBP17 deforms membranes into tubules (Figure 6C) (Frost et al., 2008; Itoh et al., 2005) that are not enriched in $PI(4,5)P_2$ (data not shown). Upon Synj1-Ptase recruitment to these F-BAR-induced tubules, there was no strong fragmentation/condensation phenotype observed (Figures 5E and 6C; Movie S7). The ENTH domain of epsin has also been reported to tubulate membranes that are enriched for $PI(4,5)P_2$ (Ford et al., 2002). When this ENTH domain was used in the heterodimerization

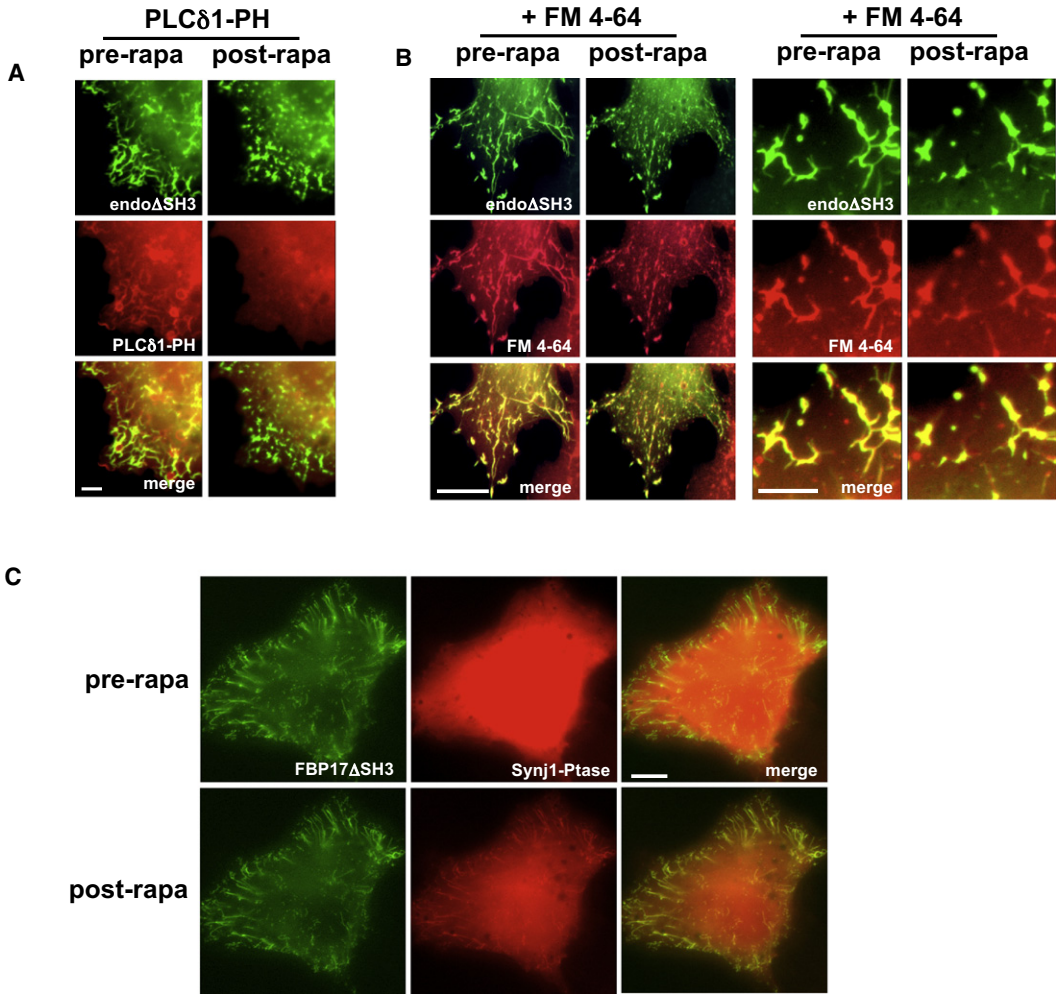

Figure 6. Characterization of Membrane Dynamics during Synj1-Induced Membrane Fission

(A) The PI(4,5)P_2 marker PLC1δ-PH localizes to endophilin-induced tubules prior to rapamycin-treatment. This marker translocates into the cytoplasm upon rapamycin-treatment demonstrating the hydrolysis of PI(4,5)P_2 by the Synj1-Ptase.

(B) Using FM4-64 as a membrane marker, fragmentation and beading of the membrane are observed.

(C) FBP17-F-BAR-induced membrane tubules do not undergo membrane reorganization upon Synj1-Ptase recruitment. Scale bars represent (A) 5 μm, (B) 10 μm (left) and 5 μm (right), and (C) 10 μm. See also Movies S5–S7.

paradigm, ENTH-labeled tubules were observed proximal to the plasma membrane and disappeared (i.e., the fluorescence became cytosolic) upon recruitment of Synj1-Ptase, somewhat reminiscent of the PH domain of PLCδ1 (data not shown). Thus, the fragmentation/condensation phenotype induced by PI(4,5)P_2 dephosphorylation appears specific for the N-BAR domain of endophilin.

Fission of Endophilin-Coated Tubules Triggered by PI(4,5)P_2 Hydrolysis Is Dynamin Dependent

Next, the dynamin dependency of the observed fission phenomenon was examined. The large GTPase dynamin has been established as an endocytic factor critical for membrane fission (Ferguson et al., 2009; Mettlen et al., 2009; Praefcke and McMahon, 2004). Staining for endogenous dynamin 2 in COS-7 cells overexpressing endophilin lacking its SH3 domain revealed that dynamin was localized at the endophilin-induced tubules, where it may have been recruited either independently [e.g., via PI(4,5)P_2] or through other endogenous BAR/SH3 proteins (Figure 7A). Preincubation of COS-7 cells expressing the endophilin and wild-type Synj1 chimerae with the dynamin inhibitor dynasore (Macia et al., 2006) resulted in the inhibition of the rapamycin-induced fragmentation/ condensation phenomenon (Figures 5E and 7B; Movie S8). To further confirm the dynamin dependency, two point mutants of dynamin 2 were used: (1) the dyn-K44A, which shows a deficiency in nucleotide binding (Praefcke and McMahon, 2004); and (2) the more potent dynamin mutant, dyn-K142A, which is defective in the conformational change observed with wild-type dynamin upon GTP hydrolysis (Marks et al., 2001). Expression of these dynamin mutants, either as a single mutation or double mutation, along with a full-length endophilin chimera and a nonfluorescent Synj1-Ptase chimera resulted in a decrease in the reduction of tubule length, albeit to a lesser degree than with the use of

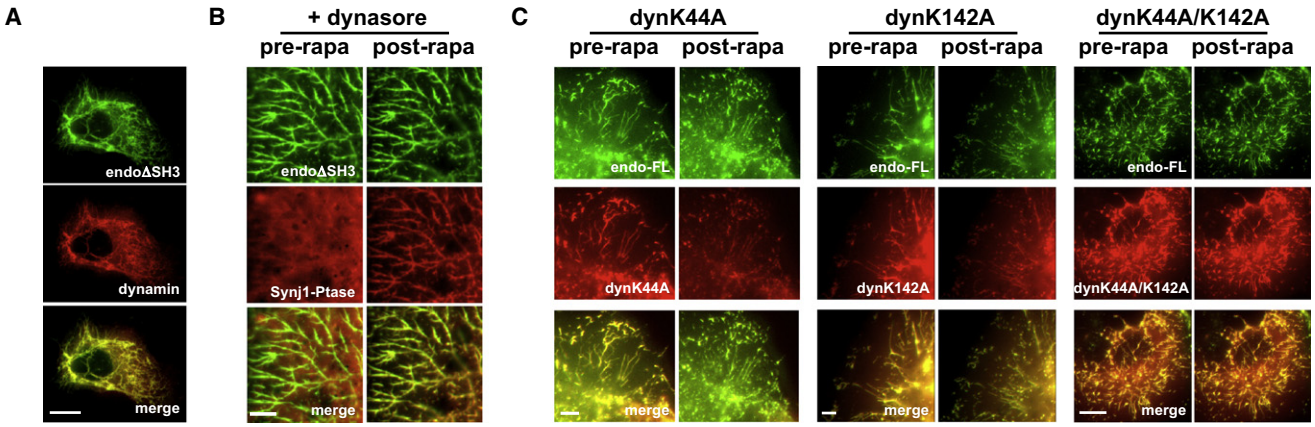

Figure 7. Synj1-Induced Membrane Fission Depends upon Dynamin

(A) Staining of COS-7 cells expressing the endoΔSH3-FRB-EGFP with anti-dynamin antibody shows that the endophilin-induced tubules are coated with endogenous dynamin 2.

(B) Pretreatment of transfected cells with the dynamin inhibitor dynasore prevents the fragmentation and condensation events induced by recruitment of Synj1-Ptase to the endophilin-induced tubules by rapamycin treatment.

(C) Effect of the single (K44A or K142A) and double (K44A/K142A) dynamin mutants on Synj1-Ptase-induced membrane fragmentation and condensation. Scale bars represent (A) 25 μm, (B) 5 μm, and (C) 5 μm (left), 5 μm (middle), and 10 μm (right). See also Movies S8 and S9.

dynasore (Figures 5E and 7C; Movie S9). Full-length endophilin, which causes the same effect as seen with the endoΔSH3 in this heterodimerization paradigm (Figure 5E), was used in these experiments to ensure proper recruitment of the overexpressed dynamin constructs to the endophilin-induced tubules via its SH3 domain. The single mutants, dyn-K44A and dyn-K142A, caused partial inhibition in the percentage of tubule length reduction (49.6% ± 3.7% and 42.9% ± 5.9%, respectively) while the double mutant, dyn-K44A/K142A, had an even stronger effect (36.9%. ± 2.7%). Altogether, these results suggest that the recruitment of Synj1 and the hydrolysis of $PI(4,5)P_2$ to PI4P by this phosphatase play a role in modulating fission of the endophilin-induced tubules and that this process is largely dependent on dynamin.

DISCUSSION

This study provides new insights into the molecular mechanisms controlling $PI(4,5)P_2$ metabolism and the potential roles of $PI(4,5)P_2$ dephosphorylation during the endocytic process. The complexity of biological processes regulated by $PI(4,5)P_2$ necessitates the fine-tuned regulation of this lipid's metabolism at the plasma membrane. Failure to achieve this regulation dramatically interferes with membrane transport to and from the cell surface, particularly the endocytic process (Di Paolo and De Camilli, 2006; Hayashi et al., 2008; Mani et al., 2007; Zoncu et al., 2007).

We have hypothesized in this study that membrane geometry may be a key factor modulating the balance between synthesis and elimination of $PI(4,5)P_2$. Cell-free assays were utilized to address the relationship between the size of substrate liposomes and $PI(4,5)P_2$ metabolism. A main conclusion drawn from our data is that $PI(4,5)P_2$ is subject to a greater turnover on small liposomes and that increased catabolism of this lipid is mediated by the Synj1-endophilin partnership. This phenomenon reflects both an increased recruitment of Synj1 onto small vesicles by endophilin and an intrinsic enzymatic preference of Synj1 for $PI(4,5)P_2$ on these small vesicles. The latter is suggested by $PI(4,5)P_2$ phosphatase assays, whereby the recruitment of Synj1 to liposomes was normalized for both large and small liposomes using the His-NiNTA interaction. Indeed, under equal recruitment conditions, there was an increased hydrolysis of $PI(4,5)P_2$ by His-Synj1 on the small liposomes. While other studies have shown that lipid hydrolysis by enzymes can be facilitated on small vesicles (Ahyayauch et al., 2005), our work dissociates the contribution of enzyme recruitment from that of the actual catalytic activity of a $PI(4,5)P_2$-metabolizing enzyme. Altogether, our results suggest that the Synj1-endophilin partnership acts as a curvature sensor to enhance $PI(4,5)P_2$ hydrolysis on highly curved membranes. This mechanism would allow for the effective elimination of $PI(4,5)P_2$ from highly curved endocytic membranes during the invagination process and from coated vesicles. In addition, although the increased phosphatase activity of Synj1 on small liposomes may appear fairly modest, previous studies on mice lacking PIP Kinase type 1 or Synj1 indicate that biochemical changes of the same magnitude in $PI(4,5)P_2$ levels correlate with significant phenotypes at the physiological and organismal levels (Cremona et al., 1999; Di Paolo et al., 2004). Furthermore, gene dosage imbalance for *Synj1*, which results in even more subtle defects in $PI(4,5)P_2$ metabolism, has major implications for brain dysfunction in such disorders as Down syndrome (Voronov et al., 2008) and Alzheimer's disease (Berman et al., 2008). Thus, the "curvature effect" on $PI(4,5)P_2$ metabolism is likely to be meaningful in the physiology of the endocytic process.

Coupling specific biochemical reactions with the acquisition of membrane curvature represents a powerful mechanism for endowing novel or differential molecular attributes to nascent membrane carriers. The disassembly of the COPI coat from Golgi-derived membrane carriers has been shown to be mediated by the hydrolysis of GTP via the small GTPase Arf1, which is promoted by a specific GTPase-activating protein, ArfGAP1,

in a curvature dependent manner (Bigay et al., 2003). ArfGAP-1 senses changes in lipid packing induced by the coat, rather than curvature per se (Antonny et al., 2005), in contrast to the BAR domain of endophilin. Indeed, experiments with liposomes of smaller diameter than 50 nm did not show decreased PIP_2 radiolabeling or increased phosphate release (data not shown), suggesting that the preference of the Synj1-endophilin partnership for more highly curved membranes most likely arises from the ability to sense curvature rather than lipid packing defects. Altogether, our study expands on previous work showing that membrane curvature plays a key role in the regulation of protein-membrane interactions underlying budding processes and coat dynamics.

While the first part of our study suggests the occurrence of a geometry-based mechanism for the efficient elimination of PI(4,5)P_2 from invaginating membranes, the second part indicates that the rapid PI(4,5)P_2-to PI4P conversion occurring on tubules may help to facilitate membrane fission. Although previously published literature is consistent with a role of synaptojanin in the fission process (Mani et al., 2007; Perera et al., 2006; Stefan et al., 2002, 2005; Sun et al., 2007), this study provides direct evidence that Synj1, via its inositol 5-phosphatase domain, can facilitate the fission of cell surface-derived membrane tubules in intact cells. Based on our data showing that the dynamin-inhibitor dynasore as well as dynamin mutants significantly impair Synj1-induced membrane fission, we conclude that PI(4,5)P_2 hydrolysis facilitates membrane fission largely in a dynamin-dependent fashion. Since dynamin binds PI(4,5)P_2 and this interaction is critical for its function, this notion may appear counterintuitive. However, recent work from a number of groups has indicated that dynamin disassembly is required for the completion of the fission process in cell-free assays (Bashkirov et al., 2008; Pucadyil and Schmid, 2008). It is possible that the PI(4,5)P_2-to-PI4P conversion by Synj1-endophilin may play a role in facilitating disassociation of dynamin from the membrane. Interestingly, dynamin itself is subject to regulation by membrane curvature, based on data showing that dynamin nucleation on membrane tubules is greatly dependent upon the diameter of these tubules (Roux et al., 2010).

Our experimental results are in agreement with a recent modeling study by Drubin, Oster, and colleagues. Indeed, these groups developed a mathematical model of endocytosis that uses membrane curvature as a central factor of endocytosis and compiles experimental knowledge attained from yeast endocytic dynamics and various mechanochemical theories to explain the spatial and temporal regulation of endocytic events (Liu et al., 2009). In this model, the feedback between membrane curvature and coupled biochemical reactions control the progression of endocytic events leading to vesicle formation and fission. In the data presented here, the activity of the endophilin-Synj1 partnership is positively regulated by membrane curvature and rapid PI(4,5)P_2 hydrolysis promotes membrane fission. It is of note that with the rapid diffusion rates of PI(4,5)P_2 in membranes (Golebiewska et al., 2008), a curvature-based mechanism to potentiate PI(4,5)P_2 hydrolysis may be futile without specific mechanisms in place to limit the diffusion of this phosphoinositide and its metabolites (Liu et al., 2009). Interestingly, Stuart McLaughlin and colleagues have recently provided evidence for the existence of a PI(4,5)P_2 "fence" at the plasma membrane of a macrophage cell line (S. McLaughlin, personal communication), further suggesting that PI(4,5)P_2 metabolism may be locally regulated.

Synj1 has been established as an important component in the machinery controlling synaptic vesicle recycling. The most prominent morphological phenotype observed in *Synj1*$^{-/-}$ neurons is the accumulation of clathrin-coated vesicles in inhibitory neurons suggesting the importance for this enzyme in the uncoating of endocytic vesicles (Cremona et al., 1999; Kim et al., 2002). However, slowed endocytic kinetics in *Synj1*$^{-/-}$ neurons (Mani et al., 2007), an accumulation of endocytic intermediates at various stages in nerve terminals from lower organisms lacking functional Synj enzymes (Harris et al., 2000; Verstreken et al., 2003) or from blockade of Synj enzymes (Gad et al., 2000), and recruitment of Synj to endocytic pits immediately prior to vesicle scission (Perera et al., 2006; Sun et al., 2007) have been reported. All these lines of evidence intimate a role of Synj1 (and its orthologs in lower organisms) prior to uncoating during the recycling process. The accumulation of coated vesicles is not incompatible with suboptimal fission since PI(4,5)P_2 is known to modulate the endocytic machinery at multiple levels. Thus, the PI(4,5)P_2-to PI4P conversion may act as a switch to facilitate and coordinate the fission and uncoating processes.

In summary, our study describes how the PI(4,5)P_2-to-PI4P conversion by Synj1 is regulated by membrane curvature and the endophilin-Synj1 partnership and that this conversion participates in regulating the dynamin-dependent membrane fission process. The recent identification of inositol 5-phosphatase OCRL as an interactor for BAR protein APPL1 suggests that our findings may apply to other protein complexes involved in membrane trafficking events in various cellular compartments (Erdmann et al., 2007). OCRL and another 5-phosphatase, SHIP2, have been reported to be recruited to clathrin-coated pits (Nakatsu et al., 2010), and, thus, may be under similar principles of regulation as Synj1, that is, by membrane curvature. Such 5-phosphatases may also cooperate with Synj1 to facilitate membrane fission.

EXPERIMENTAL PROCEDURES

Brain Cytosol, Plasmids, Antibodies, Protein Expression, and Purification

All reagents, including brain cytosols, plasmids, and antibodies, as well as protein expression and purification methods can be found in the Supplemental Experimental Procedures.

Following is a summary of the materials and methods used. Detailed methods and information can be found in the Supplemental Experimental Procedures.

Liposome Preparation

Lipids were obtained from Sigma-Aldrich, Avanti Polar Lipids, and Echelon Biosciences. Liposomes were prepared as recommended at www.avantilipids.com. The resulting liposomes were large, multilamellar vesicles/liposomes (crude liposomes). Sizing of liposomes was achieved by extrusion through polycarbonate membranes with different pore sizes. Measurement of liposome sizes can be found in the Supplemental Experimental Procedures.

Liposome Radiolabeling Assay

Folch liposomes and brain cytosol samples were incubated for 15 min at 37°C in kinase buffer and 5 mCi [γ-^{32}P]-ATP and then processed as previously described (Cremona et al., 1999), with a few modifications. Lipids were

extracted, separated by TLC, and then visualized by phosphorimaging using a Storm Imaging System (GE Heathcare).

Liposome Sedimentation Assay

Rat brain cytosol was incubated with Folch liposomes for 15 min. at either 4°C or 37°C. These reactions were then subjected to high-speed centrifugation and pellets analyzed by western blotting. For binding of purified endophilin proteins, proteins were incubated with crude liposomes with varying phospholipid compositions for 30 min at RT and then sedimented and analyzed by Coomassie staining. Blots were analyzed on the Odyssey Infrared Imaging System (LI-COR Biosciences).

PI(4,5)P_2 Phosphatase Assay

For the soluble-PI(4,5)P_2 phosphatase assay, brain cytosol and water soluble, short-chain (C6) BODIPY-labeled PI(4,5)P_2 in kinase buffer were incubated for 15 min at 37°C. The reaction products were separated by TLC, visualized under UV light and quantified using Image J software (NIH). In the PI(4,5)P_2 phosphatase time-course studies, 5% PI(4,5)P_2 liposomes were incubated with purified FLAG-Synj1 with or without endophilin at 37°C for the times specified. Levels of released phosphate were measured using the PiPer Phosphate Assay kit according to manufacturer's instructions (Invitrogen). Phosphate release was not assessed for time points below 1 min for technical reasons.

His-Synj1 Activity and Recruitment Assay

For the His-Synj1 activity assay, NiNTA liposomes in liposome buffer B, ± EDTA, were preincubated on ice. Once His-Synj1 was added, the reaction tubes were immediately incubated at 37°C for 10 min. The lipids were extracted and processed by ImageJ as in the PI(4,5)P_2 phosphatase assay. To measure the amount of His-Synj1 recruitment to NiNTA liposomes, we modified a liposome flotation assay described previously (Bigay and Antonny, 2005). Recovery of liposomes was assessed using fluorimetry. His-Synj1 levels were checked by western blot.

Fluorescence Microscopy and Live Imaging

COS-7 cells were transfected and grown on glass coverslips (Warner Instruments). For fixed staining, cells were fixed with 4% paraformaldehyde at RT. For live imaging, coverslips were placed in a Chamlide recording chamber (Life Cell Instruments, South Korea) filled with HBS solution and imaging was performed at 37°C using the Olympus IX-81 microscope using Slidebook 5.0 software (Olympus). For FM4-64 (Invitrogen) staining, cells were incubated with the dye in HBS. For the heterodimerization experiments, cells were treated with either 5 μM rapalog or 100 nM rapamycin. In experiments using dynasore, cells were preincubated with 80 μM dynasore for 20 min before rapamycin treatment. Tubule length before and after rapamycin or rapalog treatment was measured using ImageJ. For each cell recorded, the initial length of tubules before the application of rapamycin was measured by drawing a segmented thin line along the tubules (Li). The residual length of the same tubules was measured similarly from the image obtained 2 min after the application of rapamycin (Lr). The lengths of the tubules before (ΣLi) and after (ΣLr) were summated and the difference (ΣLi- ΣLr) was normalized to the total lengths of the tubules before rapamycin treatment (ΣLi).

Statistics

Statistical analyses were performed using two-tailed equal variance Student's t test or one-way ANOVA analysis with Tukey-Kramer multiple comparisons post-test.

SUPPLEMENTAL INFORMATION

Supplemental Information includes one table, three figures, Supplemental Experimental Procedures, and nine movies and can be found with this article online at doi:10.1016/j.devcel.2010.12.008.

ACKNOWLEDGMENTS

We are grateful to P. De Camilli, Yale University, for the kind gift of *Synj1*$^{-/-}$ mice and Synj1, endophilin, and FBP17 cDNAs and antibodies; T. Balla, NIH, for the PLCδ1-PH-mRFP construct; S. Grinstein, Hospital for Sick Children, Toronto, Canada, for the R-pre-mRFP construct; S. Chang, College of Medicine of the Korea University, for dynamin 2 K44A cDNAs; T. Kirchhausen, Harvard University, for dynasore; and Ariad Pharmaceuticals for providing the AP21967 rapalog. We thank E. Miller, S. McLaughlin, A. Bhalla, E. Morel, and Z. Chamoun for critical reading of the manuscript. We also thank N. Quibria for work on preliminary studies, A. Cavelli and L.B. McIntire for help with experiments, and X. Guan and M.R. Wenk for mass spectrometry analysis of liposomes. This work is funded by NIH grant R01 NS056049 and the McKnight Endowment Fund to G.D.P. and NIH grant F31 NS058096 to B.C.-I.

Received: March 16, 2009
Revised: August 27, 2010
Accepted: December 9, 2010
Published: February 14, 2011

REFERENCES

Ahyayauch, H., Villar, A.V., Alonso, A., and Goni, F.M. (2005). Modulation of PI-specific phospholipase C by membrane curvature and molecular order. Biochemistry *44*, 11592–11600.

Antonny, B., Bigay, J., Casella, J.F., Drin, G., Mesmin, B., and Gounon, P. (2005). Membrane curvature and the control of GTP hydrolysis in Arf1 during COPI vesicle formation. Biochem. Soc. Trans. *33*, 619–622.

Bashkirov, P.V., Akimov, S.A., Evseev, A.I., Schmid, S.L., Zimmerberg, J., and Frolov, V.A. (2008). GTPase cycle of dynamin is coupled to membrane squeeze and release, leading to spontaneous fission. Cell *135*, 1276–1286.

Berman, D.E., Dall'Armi, C., Voronov, S.V., McIntire, L.B., Zhang, H., Moore, A.Z., Staniszewski, A., Arancio, O., Kim, T.W., and Di Paolo, G. (2008). Oligomeric amyloid-beta peptide disrupts phosphatidylinositol-4,5-bisphosphate metabolism. Nat. Neurosci. *11*, 547–554.

Bigay, J., and Antonny, B. (2005). Real-time assays for the assembly-disassembly cycle of COP coats on liposomes of defined size. Methods Enzymol. *404*, 95–107.

Bigay, J., Gounon, P., Robineau, S., and Antonny, B. (2003). Lipid packing sensed by ArfGAP1 couples COPI coat disassembly to membrane bilayer curvature. Nature *426*, 563–566.

Chichili, G.R., and Rodgers, W. (2009). Cytoskeleton-membrane interactions in membrane raft structure. Cell. Mol. Life Sci. *66*, 2319–2328.

Cremona, O., Di Paolo, G., Wenk, M.R., Lüthi, A., Kim, W.T., Takei, K., Daniell, L., Nemoto, Y., Shears, S.B., Flavell, R.A., et al. (1999). Essential role of phosphoinositide metabolism in synaptic vesicle recycling. Cell *99*, 179–188.

Di Paolo, G., and De Camilli, P. (2006). Phosphoinositides in cell regulation and membrane dynamics. Nature *443*, 651–657.

Di Paolo, G., Moskowitz, H.S., Gipson, K., Wenk, M.R., Voronov, S., Obayashi, M., Flavell, R., Fitzsimonds, R.M., Ryan, T.A., and De Camilli, P. (2004). Impaired PtdIns(4,5)P2 synthesis in nerve terminals produces defects in synaptic vesicle trafficking. Nature *431*, 415–422.

Dittman, J., and Ryan, T.A. (2009). Molecular circuitry of endocytosis at nerve terminals. Annu. Rev. Cell Dev. Biol. *25*, 133–160.

Erdmann, K.S., Mao, Y., McCrea, H.J., Zoncu, R., Lee, S., Paradise, S., Modregger, J., Biemesderfer, D., Toomre, D., and De Camilli, P. (2007). A role of the Lowe syndrome protein OCRL in early steps of the endocytic pathway. Dev. Cell *13*, 377–390.

Ferguson, S.M., Raimondi, A., Paradise, S., Shen, H., Mesaki, K., Ferguson, A., Destaing, O., Ko, G., Takasaki, J., Cremona, O., et al. (2009). Coordinated actions of actin and BAR proteins upstream of dynamin at endocytic clathrin-coated pits. Dev. Cell *17*, 811–822.

Ford, M.G., Mills, I.G., Peter, B.J., Vallis, Y., Praefcke, G.J., Evans, P.R., and McMahon, H.T. (2002). Curvature of clathrin-coated pits driven by epsin. Nature *419*, 361–366.

Frost, A., Perera, R., Roux, A., Spasov, K., Destaing, O., Egelman, E.H., De Camilli, P., and Unger, V.M. (2008). Structural basis of membrane invagination by F-BAR domains. Cell *132*, 807–817.

Frost, A., Unger, V.M., and De Camilli, P. (2009). The BAR domain superfamily: membrane-molding macromolecules. Cell *137*, 191–196.

Gad, H., Ringstad, N., Löw, P., Kjaerulff, O., Gustafsson, J., Wenk, M., Di Paolo, G., Nemoto, Y., Crun, J., Ellisman, M.H., et al. (2000). Fission and uncoating of synaptic clathrin-coated vesicles are perturbed by disruption of interactions with the SH3 domain of endophilin. Neuron *27*, 301–312.

Gallop, J.L., Jao, C.C., Kent, H.M., Butler, P.J., Evans, P.R., Langen, R., and McMahon, H.T. (2006). Mechanism of endophilin N-BAR domain-mediated membrane curvature. EMBO J. *25*, 2898–2910.

Golebiewska, U., Nyako, M., Woturski, W., Zaitseva, I., and McLaughlin, S. (2008). Diffusion coefficient of fluorescent phosphatidylinositol 4,5-bisphosphate in the plasma membrane of cells. Mol. Biol. Cell *19*, 1663–1669.

Guo, S., Stolz, L.E., Lemrow, S.M., and York, J.D. (1999). SAC1-like domains of yeast SAC1, INP52, and INP53 and of human synaptojanin encode polyphosphoinositide phosphatases. J. Biol. Chem. *274*, 12990–12995.

Harris, T.W., Hartwieg, E., Horvitz, H.R., and Jorgensen, E.M. (2000). Mutations in synaptojanin disrupt synaptic vesicle recycling. J. Cell Biol. *150*, 589–600.

Haucke, V., and Di Paolo, G. (2007). Lipids and lipid modifications in the regulation of membrane traffic. Curr. Opin. Cell Biol. *19*, 426–435.

Hayashi, M., Raimondi, A., O'Toole, E., Paradise, S., Collesi, C., Cremona, O., Ferguson, S.M., and De Camilli, P. (2008). Cell- and stimulus-dependent heterogeneity of synaptic vesicle endocytic recycling mechanisms revealed by studies of dynamin 1-null neurons. Proc. Natl. Acad. Sci. USA *105*, 2175–2180.

Hurley, J.H., and Meyer, T. (2001). Subcellular targeting by membrane lipids. Curr. Opin. Cell Biol. *13*, 146–152.

Itoh, T., Erdmann, K.S., Roux, A., Habermann, B., Werner, H., and De Camilli, P. (2005). Dynamin and the actin cytoskeleton cooperatively regulate plasma membrane invagination by BAR and F-BAR proteins. Dev. Cell *9*, 791–804.

Jost, M., Simpson, F., Kavran, J.M., Lemmon, M.A., and Schmid, S.L. (1998). Phosphatidylinositol-4,5-bisphosphate is required for endocytic coated vesicle formation. Curr. Biol. *8*, 1399–1402.

Kim, W.T., Chang, S., Daniell, L., Cremona, O., Di Paolo, G., and De Camilli, P. (2002). Delayed reentry of recycling vesicles into the fusion-competent synaptic vesicle pool in synaptojanin 1 knockout mice. Proc. Natl. Acad. Sci. USA *99*, 17143–17148.

Lee, S.Y., Wenk, M.R., Kim, Y., Nairn, A.C., and De Camilli, P. (2004). Regulation of synaptojanin 1 by cyclin-dependent kinase 5 at synapses. Proc. Natl. Acad. Sci. USA *101*, 546–551.

Liu, J., Sun, Y., Drubin, D.G., and Oster, G.F. (2009). The mechanochemistry of endocytosis. PLoS Biol. *7*, e1000204.

Macia, E., Ehrlich, M., Massol, R., Boucrot, E., Brunner, C., and Kirchhausen, T. (2006). Dynasore, a cell-permeable inhibitor of dynamin. Dev. Cell *10*, 839–850.

Mani, M., Lee, S.Y., Lucast, L., Cremona, O., Di Paolo, G., De Camilli, P., and Ryan, T.A. (2007). The dual phosphatase activity of synaptojanin1 is required for both efficient synaptic vesicle endocytosis and reavailability at nerve terminals. Neuron *56*, 1004–1018.

Marks, B., Stowell, M.H., Vallis, Y., Mills, I.G., Gibson, A., Hopkins, C.R., and McMahon, H.T. (2001). GTPase activity of dynamin and resulting conformation change are essential for endocytosis. Nature *410*, 231–235.

Masuda, M., Takeda, S., Sone, M., Ohki, T., Mori, H., Kamioka, Y., and Mochizuki, N. (2006). Endophilin BAR domain drives membrane curvature by two newly identified structure-based mechanisms. EMBO J. *25*, 2889–2897.

McLaughlin, S., and Murray, D. (2005). Plasma membrane phosphoinositide organization by protein electrostatics. Nature *438*, 605–611.

McPherson, P.S., Garcia, E.P., Slepnev, V.I., David, C., Zhang, X., Grabs, D., Sossin, W.S., Bauerfeind, R., Nemoto, Y., and De Camilli, P. (1996). A presynaptic inositol-5-phosphatase. Nature *379*, 353–357.

Mettlen, M., Pucadyil, T., Ramachandran, R., and Schmid, S.L. (2009). Dissecting dynamin's role in clathrin-mediated endocytosis. Biochem. Soc. Trans. *37*, 1022–1026.

Milosevic, I., Sorensen, J.B., Lang, T., Krauss, M., Nagy, G., Haucke, V., Jahn, R., and Neher, E. (2005). Plasmalemmal phosphatidylinositol-4,5-bisphosphate level regulates the releasable vesicle pool size in chromaffin cells. J. Neurosci. *25*, 2557–2565.

Nakatsu, F., Perera, R.M., Lucast, L., Zoncu, R., Domin, J., Gertler, F.B., Toomre, D., and De Camilli, P. (2010). The inositol 5-phosphatase SHIP2 regulates endocytic clathrin-coated pit dynamics. J. Cell Biol. *109*, 307–315.

Perera, R.M., Zoncu, R., Lucast, L., De Camilli, P., and Toomre, D. (2006). Two synaptojanin 1 isoforms are recruited to clathrin-coated pits at different stages. Proc. Natl. Acad. Sci. USA *103*, 19332–19337.

Peter, B.J., Kent, H.M., Mills, I.G., Vallis, Y., Butler, P.J., Evans, P.R., and McMahon, H.T. (2004). BAR domains as sensors of membrane curvature: the amphiphysin BAR structure. Science *303*, 495–499.

Pike, L.J. (2009). The challenge of lipid rafts. J. Lipid Res. Suppl. *50*, S323–S328.

Praefcke, G.J., and McMahon, H.T. (2004). The dynamin superfamily: universal membrane tubulation and fission molecules? Nat. Rev. Mol. Cell Biol. *5*, 133–147.

Pucadyil, T.J., and Schmid, S.L. (2008). Real-time visualization of dynamin-catalyzed membrane fission and vesicle release. Cell *135*, 1263–1275.

Ramachandran, R., and Schmid, S.L. (2008). Real-time detection reveals that effectors couple dynamin's GTP-dependent conformational changes to the membrane. EMBO J. *27*, 27–37.

Ringstad, N., Nemoto, Y., and De Camilli, P. (1997). The SH3p4/Sh3p8/SH3p13 protein family: binding partners for synaptojanin and dynamin via a Grb2-like Src homology 3 domain. Proc. Natl. Acad. Sci. USA *94*, 8569–8574.

Ringstad, N., Nemoto, Y., and De Camilli, P. (2001). Differential expression of endophilin 1 and 2 dimers at central nervous system synapses. J. Biol. Chem. *276*, 40424–40430.

Roux, A., Koster, G., Lenz, M., Sorre, B., Manneville, J.B., Nassoy, P., and Bassereau, P. (2010). Membrane curvature controls dynamin polymerization. Proc. Natl. Acad. Sci. USA *107*, 4141–4146.

Schuske, K.R., Richmond, J.E., Matthies, D.S., Davis, W.S., Runz, S., Rube, D.A., van der Bliek, A.M., and Jorgensen, E.M. (2003). Endophilin is required for synaptic vesicle endocytosis by localizing synaptojanin. Neuron *40*, 749–762.

Singer-Kruger, B., Nemoto, Y., Daniell, L., Ferro-Novick, S., and De Camilli, P. (1998). Synaptojanin family members are implicated in endocytic membrane traffic in yeast. J. Cell Sci. *111*, 3347–3356.

Srinivasan, S., Seaman, M., Nemoto, Y., Daniell, L., Suchy, S.F., Emr, S., De Camilli, P., and Nussbaum, R. (1997). Disruption of three phosphatidylinositol-polyphosphate 5-phosphatase genes from Saccharomyces cerevisiae results in pleiotropic abnormalities of vacuole morphology, cell shape, and osmohomeostasis. Eur. J. Cell Biol. *74*, 350–360.

Stefan, C.J., Audhya, A., and Emr, S.D. (2002). The yeast synaptojanin-like proteins control the cellular distribution of phosphatidylinositol (4,5)-bisphosphate. Mol. Biol. Cell *13*, 542–557.

Stefan, C.J., Padilla, S.M., Audhya, A., and Emr, S.D. (2005). The phosphoinositide phosphatase Sjl2 is recruited to cortical actin patches in the control of vesicle formation and fission during endocytosis. Mol. Cell. Biol. *25*, 2910–2923.

Sun, Y., Carroll, S., Kaksonen, M., Toshima, J.Y., and Drubin, D.G. (2007). PtdIns(4,5)P2 turnover is required for multiple stages during clathrin- and actin-dependent endocytic internalization. J. Cell Biol. *177*, 355–367.

Traub, L.M. (2005). Common principles in clathrin-mediated sorting at the Golgi and the plasma membrane. Biochim. Biophys. Acta *1744*, 415–437.

van Rheenen, J., Achame, E.M., Janssen, H., Calafat, J., and Jalink, K. (2005). PIP2 signaling in lipid domains: a critical re-evaluation. EMBO J. *24*, 1664–1673.

Verstreken, P., Koh, T.W., Schulze, K.L., Zhai, R.G., Hiesinger, P.R., Zhou, Y., Mehta, S.Q., Cao, Y., Roos, J., and Bellen, H.J. (2003). Synaptojanin is recruited by endophilin to promote synaptic vesicle uncoating. Neuron *40*, 733–748.

Voronov, S.V., Frere, S.G., Giovedi, S., Pollina, E.A., Borel, C., Zhang, H., Schmidt, C., Akeson, E.C., Wenk, M.R., Cimasoni, L., et al. (2008). Synaptojanin 1-linked phosphoinositide dyshomeostasis and cognitive deficits in mouse models of Down's syndrome. Proc. Natl. Acad. Sci. USA *105*, 9415–9420.

Weissenhorn, W. (2005). Crystal structure of the endophilin-A1 BAR domain. J. Mol. Biol. *351*, 653–661.

Yeung, T., Terebiznik, M., Yu, L., Silvius, J., Abidi, W.M., Philips, M., Levine, T., Kapus, A., and Grinstein, S. (2006). Receptor activation alters inner surface potential during phagocytosis. Science *313*, 347–351.

Zoncu, R., Perera, R.M., Sebastian, R., Nakatsu, F., Chen, H., Balla, T., Ayala, G., Toomre, D., and De Camilli, P.V. (2007). Loss of endocytic clathrin-coated pits upon acute depletion of phosphatidylinositol 4,5-bisphosphate. Proc. Natl. Acad. Sci. USA *104*, 3793–3798.